Biochimica et Biophysica Acta, 1148 (1993) 197–208

BBAMEM 75931

Computer simulation of lipid diffusion in a two-component bilayer. The effect of adsorbing macromolecules

David A. Pink, K.S. Ramadurai and J.R. Powell

Department of Physics, St. Francis Xavier University, Antigonish (Canada)

(Received 20 November 1992)

Key words: Macromolecule; Bilayer; Computer simulation; Lipid diffusion; Diffusion coefficient

We have modelled the effects of macromolecular adsorption upon lipid lateral diffusion in a two-component lipid bilayer or monolayer, which is at a temperature above both of the main transition temperatures. One set of lipids (binders, b) can bind to the macromolecules with a free energy of binding, F_B, while the other set does not bind (non-binders, nb). We assumed that no phase separation of the lipids occurs in the absence of adsorbed macromolecules. We represented the lipid bilayer/monolayer by a triangular lattice, each site of which is occupied by a lipid molecule. Adsorbed macromolecules were represented by hexagons covering n_H sites, and we defined a probability per unit of time, p, that a hexagon attempts to adsorb onto the lattice. We considered two sizes of hexagons, $n_H = 7$ (Size-1) and $n_H = 19$ (Size-2) and disallowed or permitted adsorbed hexagons to move laterally on the lattice. We calculate the lipid relative diffusion coefficients, D_{nb}, and D_b, for three characteristic time-regimes, (i) $\tau_c \ll \tau_a$, (ii) $\tau_c \approx \tau_a$ and (iii) $\tau_c \gg \tau_a$, where τ_c and τ_a are the times for proteins to adsorb/desorb or for lipids to move from site to site, respectively. We obtain analytical expressions for D_{nb} and D_b in the first case and calculate them using computer simulation in the other two cases. We found that (i) D_α(iii) $\leq D_\alpha$(ii) $\leq D_\alpha$(i) (α = nb, b); (ii) D_α could display a shoulder as a function of F_B for low values of p; (iii) compared to cases in which lateral diffusion was disallowed, the lateral diffusion of absorbed hexagons appeared to have little effect on D_{nb}, but could cause D_b to increase by 50%. (iv) Scatter in the calculated values of D via simulation appeared to be largest for Size-1 hexagons, and could be understood as a consequence of the large interfacial region between areas free of hexagons and areas 'covered' by hexagons. Our results suggest that it is advisable to measure D_b, since D_{nb} might show little change from 1.0 for the values of F and p appropriate to the system being studied.

Introduction

An understanding of the process of protein adsorption onto the surface of lipid bilayer membranes or monolayers is a challenge to both experimentalists and theorists. While much work has been done on protein adsorption at solid/liquid interfaces [1–5], relatively little work has been done on the adsorption of proteins onto lipid bilayer membranes or monolayers [6–11], and then it has not been concerned with a calculation of diffusion coefficients [12,13]. The intention of this paper is to introduce and study a model of extrinsic proteins interacting with a lipid bilayer membrane or a lipid monolayer in order to see the effect of protein adsorption upon lipid lateral diffusion coefficients. In recent years, a number of theoretical papers appear to have understood the decrease of tracer or protein lateral diffusion coefficients with increasing integral protein concentration in a lipid bilayer. These papers have used either lattice models and Monte Carlo methods to simulate diffusion [14,15], or else related the diffusion coefficient to a pair correlation function which was then calculated [16]. It was found that there was excellent agreement between all approaches [17–20]. It was also found that experimental data on protein self-diffusion could be understood by introducing an attractive interaction between model proteins (Ref. 21; see also Refs. 22, 23). Recently, the effect of different concentrations of polymerized lipids ('macrolipids') upon the lateral diffusion coefficients of labelled lipid molecules and macrolipids was modelled and the results compared well with measurements [24]. These successes support the view that Monte Carlo simulation methods can be used in appropriate circumstances to model lateral diffusion in the plane of a bilayer or a monolayer.

Here, we will model the lateral diffusion of lipid molecules in the plane of a lipid bilayer or monolayer, onto which macromolecules, e.g., proteins, are adsorbing/desorbing from a bulk in contact with the inter-

Correspondence to: D.A. Pink, Department of Physics, St. Francis Xavier University, Antigonish, Nova Scotia, Canada, B2G 1C0.

face. Our intention is to calculate how such macromolecules affect the relative diffusion coefficients of lipid molecules in the plane of the bilayer. Clearly, this process introduces an aspect not present in the models of the movement of integral proteins in lipid bilayers. In the latter case the rate of change of protein configurations in the bilayer is determined by the diffusion coefficient of proteins in the plane of the bilayer. Generally, this is less than that of the lipids, so that the important parameter is the protein concentration in the bilayer. The correlation time for protein configurations is relatively long compared to the time to move a distance equal to the diameter of a lipid molecule. In the case considered here, an important parameter is not only the concentration of macromolecules adsorbed onto the surface, but also the rate of adsorption/desorption. The latter is determined not by the viscosity of the bilayer/monolayer, but by the binding energy of the macromolecules to the interface and by the density of macromolecules in the bulk which determines their flux onto the interface.

In the next section, we describe the model that we will use, describe the computer simulation procedure, and discuss time-, length-, rate- and energy-scales. We then present the results of computer simulations, and discuss them.

Theory

(i) The model

We represent the outer half of the lipid bilayer by a triangular lattice, with periodic boundary conditions, each site of which can be occupied either by a 'lipid molecule' which binds the macromolecule in question, ('binders') or by one which does not ('non-binders'). We assume that the hydrocarbon chains of both types of lipids are essentially identical. Thus, a bilayer made up of a mixture of DMPC (non-binders) and DMPG (binders) could serve as a membrane to study the adsorption of poly(L-lysine). The plane of the membrane is assumed to be in contact with an aqueous solution which contains macromolecules, such as proteins. These macromolecules can impinge upon the surface of the membrane, thereby interacting with it. The free energy of interaction can lead to the molecules being bound on the surface (adsorbed) and subsequently being desorbed if the binding energy is sufficiently small. We assume that only monolayer coverage of the membrane surface by macromolecules is attained [25]. We represent the adsorption 'footprint' of a macromolecule onto the bilayer surface by a hexagon which covers seven lattice sites, with the hexagon centre at one site and its vertices at the other six. Both binders and non-binders can be under such a hexagon. A binder under such a hexagon may be bound to the hexagon or not. The total binding energy of an adsorbed macromolecule is proportional to the number of binders, under the hexagon, which are actually bound to the hexagon.

Lateral movement of lipid molecules is achieved by allowing them to move from site to site by effecting an exchange with one of their nearest neighbour lipids: any two nearest neighbour lipids can interchange their positions unless one, or both, of them is bound to a hexagon. We shall consider the two cases in which an adsorbed hexagon is constrained to be laterally immobile on the plane of the bilayer, or may move laterally taking with it those lipids to which it is bound. We assume that the temperature of the system is such that both types of lipid are in their 'fluid' states, so that we need not concern ourselves with phase transitions or phase separation, except for the possible sequestering of binders under adsorbed hexagons [9,26].

(ii) Computer simulation

We will use the standard Metropolis Monte Carlo algorithm [20]. In the course of the simulation, thermodynamic quantities of interest are averaged over an appropriate number of Monte Carlo steps. One Monte Carlo step involves, first, attempting to adsorb a hexagon; second, attempting to desorb hexagons by breaking bonds which have arisen when a hexagon binds to a binder; and, finally, attempting to move all lipids, and all bound hexagons, together with the lipids to which they are bound, if this is allowed. In order to carry this out we need to specify (i) the probability, per Monte Carlo step, p, that a hexagon centre will attempt to be adsorbed onto a lattice site and (ii) the free energy of binding divided by kT, F_B, ($F_B \leq 0$) between a hexagon and a binder. T is the absolute temperature and k is Boltzmann's constant. With these specified, one Monte Carlo step consists of the following:

(a) A site is randomly selected and a random number, R, $0 \leq R < 1$, is chosen. If $R \leq p$ and if that site and all of its six nearest neighbours are not already occupied by a hexagon, and if at least one of those seven sites is occupied by a binder, then the hexagon is placed there and all binders on those sites are considered 'bound' (to that hexagon). This procedure is repeated for all sites of the lattice.

(b) All hexagons are visited once and only once using a random sequence. Any unbound binder which is under a hexagon becomes bound, since the energy of the system is thereby decreased. One attempt each is then made to unbind each bound binder (including those which became bound in this Monte Carlo step as described above) which is under that hexagon. For each such bound binder, a random number, R', $0 \leq R' < 1$ is chosen. If $R' \leq \exp(+F_B)$ then that binder becomes unbound. If, at the end of this step, a hexagon is bound to no binder, then it is desorbed and removed

from the lattice. It should be noted that we are not attempting to unbind all the bound binders under a given hexagon, collectively, but rather we attempt to carry this out individually for each bound binder.

(c) All non-binders and binders are visited again in a random sequence. If the choice is a bound binder then the next choice is made. If an unbound binder or a non-binder is chosen, then one of its six nearest neighbour sites is chosen randomly. If the object at this site is an unbound binder or a non-binder, then the two objects interchange their position.

(d) In cases in which hexagons are permitted to move laterally in the plane of the bilayer, all hexagons are visited in a random sequence. One of the six directions is chosen randomly and an attempt is made to translate a hexagon, together with the lipids which are bound to it, by one lattice constant. This attempt is successful if, in so moving, the hexagon does not occupy sites already occupied by another hexagon.

The vector distance moved in this way by an unbound lipid in (c) or by a bound lipid in (d) is added to the total vector distance moved by the object which was moved, but nothing is added to the total vector distance moved by the object which was occupying the nearest neighbour site, unless that, too, was a bound lipid moved during the movement of an adsorbed hexagon. Thus, let an object visited at the M-th Monte Carlo step be labelled i. Let it be initially at site $\mathbf{r}$ and let it have moved a total vector distance of $\mathbf{R}(i)$ from the start of the simulation up to, and including, step M–1. Let the nearest neighbour site at $\mathbf{r}'$ be occupied by the object j which has moved a vector distance $\mathbf{R}(j)$ also during M–1 Monte Carlo steps. If the two objects can be interchanged, then after the exchange, object i is at $\mathbf{r}'$ and has moved a vector distance $\mathbf{R}(i) + (\mathbf{r}' - \mathbf{r})$, while object j is now at $\mathbf{r}$ and has moved a distance $\mathbf{R}(j)$.

If we average $R(i)^2$ separately over all binders and non-binders for a sufficient number of Monte Carlo steps then we will obtain $\langle r^2 \rangle_b$ and $\langle r^2 \rangle_{nb}$ respectively. The relative diffusion coefficient (in units of the lattice constant, a^2) is given by

$$D_\alpha = \langle r^2 \rangle_\alpha / M, \quad \alpha = b, nb \tag{1}$$

where b and nb denote 'binder' and 'non-binder'. It is these quantities which we will calculate and study.

(iii) Relative time scales

There are three time scales in the process of protein adsorption at lipid bilayer interfaces, as described here, and we now consider their relative magnitudes and their effect upon lipid lateral diffusion: (a) The characteristic time, τ_a, for a lipid to move a distance equal to the average lipid-lipid distance. In cases where we permit lateral movement of adsorbed proteins on the bilayer, there will be the characteristic time for it to move through one average lipid-lipid distance. Because of the weak dependence of two-dimensional mobility upon the mass of the moving object [27], this time is approximately τ_a unless the adsorbed protein is some orders of magnitude larger than a single lipid molecule; (b) the characteristic time taken, τ_b, for an unbound protein to traverse a region of non-zero bilayer-protein interaction adjacent to the bilayer, and either impinge upon the bilayer or move away from the bilayer and then leave this interaction region; (c) the characteristic times, τ_{c1} and τ_{c2}, for a protein to form a bound state with a (binder) lipid molecule and to make a transition from such a bound state to an unbound state, respectively.

Here we assume that the thickness of the region adjacent to the bilayer within which the interaction between a protein and the bilayer surface is non-negligible, is effectively zero. This assumes that $\tau_b = 0$. We cannot, however, dismiss as easily the possible interplay between the times characteristic of (a) and (c), even if we assume that there is only one characteristic time associated with the latter, $\tau_{c1} = \tau_{c2} = \tau_c$. We can, however, make the following observations: If $\tau_c \gg \tau_a$ then the diffusing lipids will see an essentially static distribution of adsorbed proteins with a given average surface coverage, while if $\tau_c \ll \tau_a$, they will move through a distribution of proteins which will be a very fast averaging over all possible distributions having a fixed average surface coverage. These two cases essentially decouple the dynamics of protein adsorption and lipid lateral movement. Indeed, the second case can simply be treated by considering the probabilities of single-site occupancy by proteins. The most difficult case, however, is when $\tau_c \approx \tau_a$ and it is this case which we will concentrate on while presenting results for the other two cases.

(iv) Fast protein exchange $\tau_c \ll \tau_a$

We can easily obtain analytic expressions for binder and non-binder relative diffusion coefficients, D_b and D_{nb}, if we assume that, because of the fast exchange of proteins at the bilayer surface, there is no correlation between the positions at which there are bound binders. In this case, the average mean square distance traversed on a lattice in M Monte Carlo steps, and, accordingly, the diffusion coefficient are given by,

$$\langle r^2 \rangle = a^2 PM$$

$$D = a^2 P \tag{2}$$

where a is the lattice constant and P is the (assumed time- and position-independent) probability of an object moving from a site to a nearest neighbour site. Let the concentration of non-binders be c (fraction of

lipids which are non-binders). Then, if the free energy of binding divided by kT (per binder) is $F_B \leq 0$, this mean field approximation yields

$$P_{nb} = c + (1-c)\left(1 - f_A(1-e^{F_B})\right)$$

$$P_b = \left(1 - f_A(1-e^{F_B})\right)P_{nb} \tag{3}$$

where f_A is the average surface area covered by the adsorbing proteins,

$$f_A = n_H N_H / N \tag{4}$$

where N_H is the average number of hexagons on the surface, n_H is the number of sites occupied by one hexagon and N is the number of lattice sites. Clearly, f_A is determined by F_B and by p, the probability per step that a hexagon will attempt to adsorb onto the lattice. These analytical expressions will be compared to the results of our simulations.

It should be noted that we have specified f_A and F_B in Eqn. 3. In order to make comparisons with our computer simulation results, we must be able to choose a value of p so that we can obtain the f_A assumed, no matter how small F_B is. Although, as a probability, $p \leq 1$, there is no a priori reason in our simulations why we may make only one attempt per Monte Carlo step to adsorb a hexagon centre at a particular site. When it is realized that this exchange rate regime can correspond to as many attempts as we wish per Monte Carlo step, then we can always find a value of p for any given pair f_A and F_B.

(v) Slow protein exchange $\tau_c \gg \tau_a$

In order to model the case in which the rate at which desorption is attempted is very much slower than the time characterizing one Monte Carlo step ($\tau_c \gg \tau_a$), we distributed a static hexagon configuration on the lattice. All binders under hexagons were bound for all Monte Carlo steps, and all binders which subsequently moved to lie under hexagons became bound for all further steps. The hexagons were adsorbed as described above, until a preselected value of surface coverage by adsorbed hexagons, f_A, was achieved. This way of creating a static distribution of hexagons biases the distribution of the hexagons adsorbed late in the procedure compared to the distribution at the start of the procedure. If an unbiased distribution is required then lateral movement of hexagons should be permitted so that the system can relax. However, in these cases we have assumed that we can ignore lateral movement of adsorbed proteins and so have not permitted such hexagon movement. Accordingly, the surface distribution of hexagons should correctly represent protein adsorption with no substantial subsequent lateral motion. We have studied the effect of hexagon lateral diffusion in other cases.

(vi) Length, diffusion time and rate scales

We have assumed that the lipid bilayer is in a fluid lipid phase at a temperature sufficiently far above the main transition temperatures of the two kinds of lipid. Since each lattice site represents the cross-sectional area of a lipid molecule, then each site corresponds to an area of ~ 0.6 nm^2 [28,29], with the lattice constant, a, representing a length of ~ 0.83 nm. In order to identify the length of time elapsed for each Monte Carlo step, we equate the two expressions for the average mean square distance moved in a random walk of M Monte Carlo steps on the (hexagon-free) lattice, in an elapsed time of Δt:

$$\langle r^2 \rangle = 1/4 D_L \Delta t = a^2 M \tag{5}$$

If we choose $D_L \approx 0.55 \cdot 10^{-8}$ cm^2/s [30,31], then we find that

$$\Delta t \approx 5 \cdot 10^{-7} M \tag{6}$$

so that one Monte Carlo step corresponds to $\sim 5 \cdot 10^{-7}$ s. Here we have assumed that all Monte Carlo steps represent elapsed time of equal magnitude.

Finally, using our assumption that each lattice site corresponds to one lipid molecule of area ~ 0.6 nm^2 and that one Monte Carlo step corresponds to $\sim 5 \cdot 10^{-7}$ s, we can calculate the rate, R_M, at which macromolecules are impinging upon the surface of the membrane. For a given value of p, for cases in which only one attempt is made, per Monte Carlo step, to locate a hexagon centre at a given site, we obtain

$$R_M \approx 0.33 p \cdot 10^7 \text{ molecules/nm}^2 \text{ per s} \tag{7}$$

If more than one attempt is made per Monte Carlo step, then Eqn. 7 is multiplied by that number. The 'footprint' of each molecule corresponds to $\sim 0.6\, n_H$ nm^2.

(vii) Energy scales

The Boltzmann factor in equilibrium statistical mechanics can be written as

$$d_B e^{-E_B/kT} = e^{-F_B}$$

$$F_B = \mathcal{F}_B / kT \tag{8}$$

$$\mathcal{F}_B = E_B - kT \ln d_B$$

where E_B and d_B are the energy and degeneracy of the bound state relative to the unbound state. E_B is therefore negative and it is plausible that $d_B < 1$, since the unbound state should possess higher entropy than the bound state. Accordingly, although E_B might be very negative, F_B could be small if d_B is small.

If Boltzmann's constant is taken as $k = 1.3806$ and the absolute temperature, T, is written in units of 10^3

K, then the units of $\mathscr{F}_B$ will be 10^{-13} erg/bound state. If we choose the temperature to be 30°C ($T = 0.3032$) then we can relate $\mathscr{F}_B$ to our choices of F_B:

$$\mathscr{F}_B = 2.613F_B \ (10^{-2} \text{ eV})$$

$$\mathscr{F}_B = 2.52F_B \ (\text{kJ/mol}) \qquad (9)$$

Results

We studied lipid diffusion with hexagons of two sizes, $n_H = 7$ and $n_H = 19$. We refer to these as Size-1 and Size-2 hexagons. In order to study the cases $\tau_c \approx \tau_a$ and $\tau_c \gg \tau_a$, we performed simulations on $(60)^2$ triangular lattices with periodic boundary conditions. We ran each simulation for between 500 and 5000 Monte Carlo steps with initialization of between 50 and 2000 steps.

We chose two cases for the concentration of non-binders: $c = 0.8$ and $c = 0.5$ in order to display a range of results. We chose four values of p: $p = 0.001$, $p = 0.007$, $p = 0.05$ and $p = 0.1$ for the case $\tau_c \approx \tau_a$. To study the case $\tau_c \ll \tau_a$ we also performed simulations for other values of p in order to show how the relative diffusion coefficients varied with the free energy of binding divided by kT, F_B, at a fixed average surface coverage by adsorbed hexagons, f_A. In what follows, Figs. 1 to 9 describe cases in which the hexagon is not allowed to move in the plane of the bilayer, while Figs. 10 to 12 describe cases in which this is allowed.

Figs. 1 and 2 show the dependence of the relative diffusion coefficients, D_b and D_{nb}, for Size-1 hexagons ($n_H = 7$) and non-binder concentrations $c = 0.5$ and $c = 0.8$, for F_B ranging from 0 to -3. There are two kinds of result. When p is sufficiently small, then, for small F_B, the fractional area covered by the hexagons, f_A, rises very slowly with decreasing F_B. As F_B decreases further f_A rises more rapidly followed by a decreasing slope as saturation is approached. The consequence of this for the relative diffusion coefficients is that they exhibit a shoulder for small values of F_B, then decrease more rapidly as F_B decreases, followed by a levelling out as F_B becomes very negative. This behaviour can be seen for both $c = 0.5$ and $c = 0.8$ with $p = 0.001$ and $p = 0.007$.

For higher values of p, the shoulders in D_b and D_{nb} are absent, as is the initial small increase of f_A, for

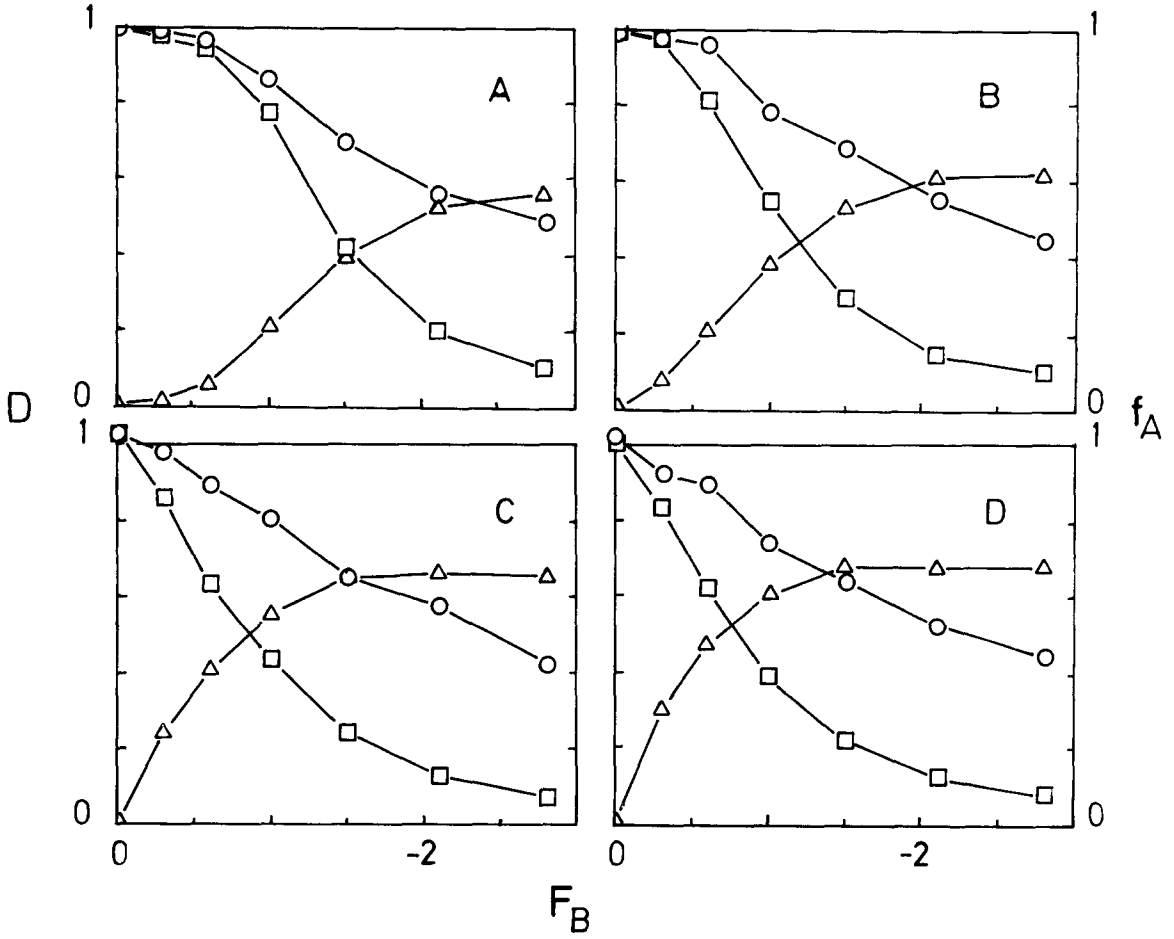

Fig. 1. Size-1 hexagons. Hexagon lateral diffusion disallowed. Relative diffusion coefficients, D_{nb} (○) and D_b (□), and f_A (△) as functions of F_B for $c = 0.5$. (A) $p = 0.001$. (B) $p = 0.007$. (C) $p = 0.05$. (D) $p = 0.1$.

small F_B. The diffusion coefficients decrease at rates which approach zero as F_B increases. This behaviour is seen for $c = 0.5$ and $c = 0.8$ with $p = 0.05$ and $p = 0.1$.

Fig. 3 shows diffusion coefficients for Size-1 hexagons and compares results for the three time-scale regimes for three values of f_A, and for non-binder concentration, $c = 0.5$. The upper sets of solid and dashed curves (a) show D_{nb} and D_b, respectively, for $f_A = 0.207$, $f_A = 0.4$ and $f_A = 0.558$ for the case $\tau_c \ll \tau_a$ using Eqn. 3, while the data points, connected by straight lines, are the results of simulations carried out at approximately the same fractional area coverages. The fluctuations in the latter reflect the fact that they are for values of f_A which may differ by a few percent. It is clear that when the system is in the fast protein exchange regime, the relative diffusion coefficients are substantially larger than in those cases where $\tau_c \approx \tau_a$. The observation that, for low value of F_B and larger values of p, the two cases give similar results simply reflects the fact that under those conditions hexagons are adsorbing/desorbing relatively quickly compared to the lateral diffusion time scale.

The lowest sets of horizontal solid and dashed lines (b) are the results of simulations carried out at the f_A values shown, by the procedure described in part (v) of the last section designed to simulate the case $\tau_c \gg \tau_a$. It is clear that for given values of F_B and f_A, the following relations hold:

$$D_\alpha(\tau_c \gg \tau_a) \leq D_\alpha(\tau_c \approx \tau_a) \leq D_\alpha(\tau_c \ll \tau_a) \tag{10}$$

where α = b or nb.

Fig. 4 compares cases for Size-1 hexagons for given values of c and F_B, when $\tau_c \approx \tau_a$, as functions of p, the probability that a hexagon will attempt to adsorb on a randomly selected set of seven sites. This is perhaps the data most closely related to experiments which can be carried out. It can be seen that there is a range of p values where $D_{nb} > 0.9$. It is only when the free energy of binding becomes strong (i.e., $\exp(F_B) \ll 1$) that D_{nb} falls below about 0.9. The same cannot be said of D_b, which displays a marked decrease in all cases shown. Of course, if p is very large and F_B not too small, then both diffusion coefficients will be small. Conversely, as

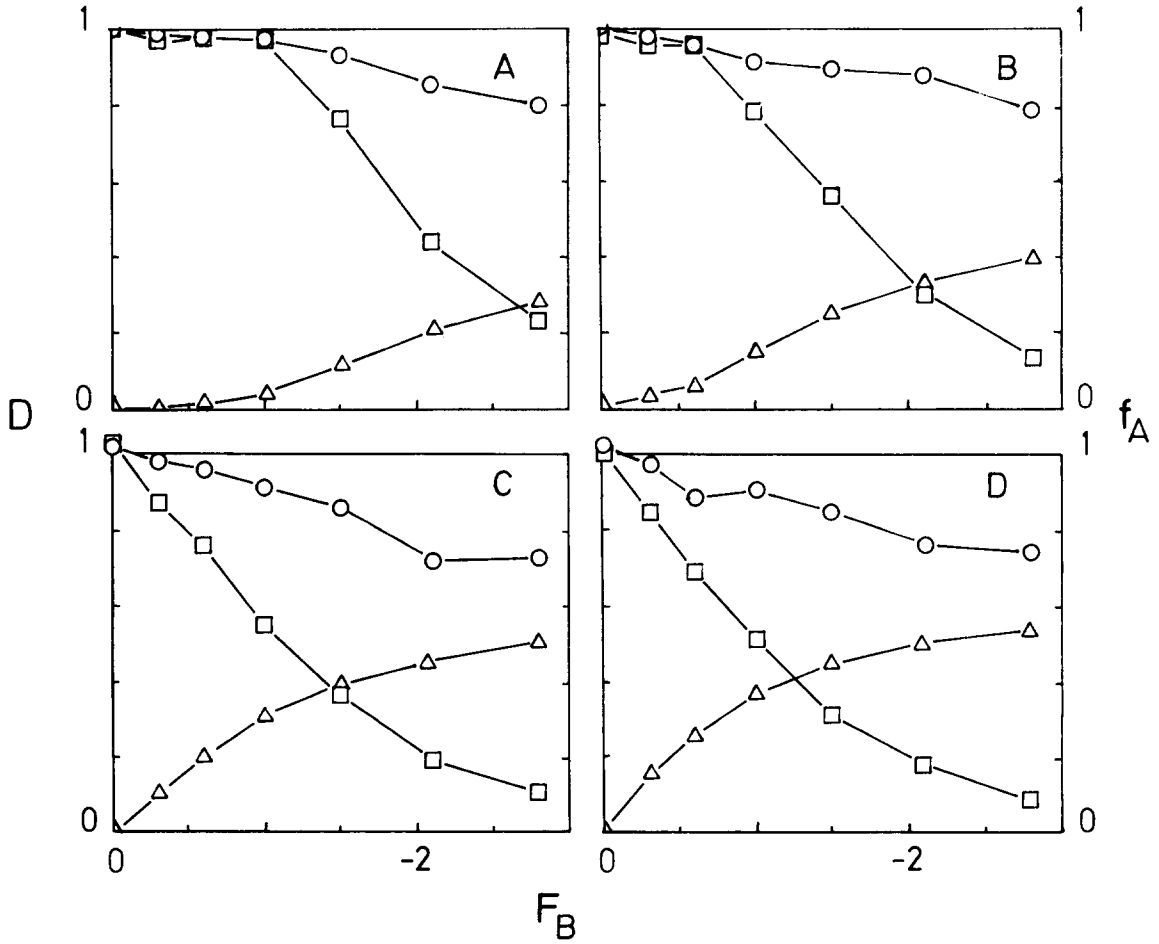

Fig. 2. Size-1 hexagons. Hexagon lateral diffusion disallowed. Relative diffusion coefficients, D_{nb} (○) and D_b (□), and f_A (△) as functions of F_B for $c = 0.8$. (A) $p = 0.001$. (B) $p = 0.007$. (C) $p = 0.05$. (D) $p = 0.1$.

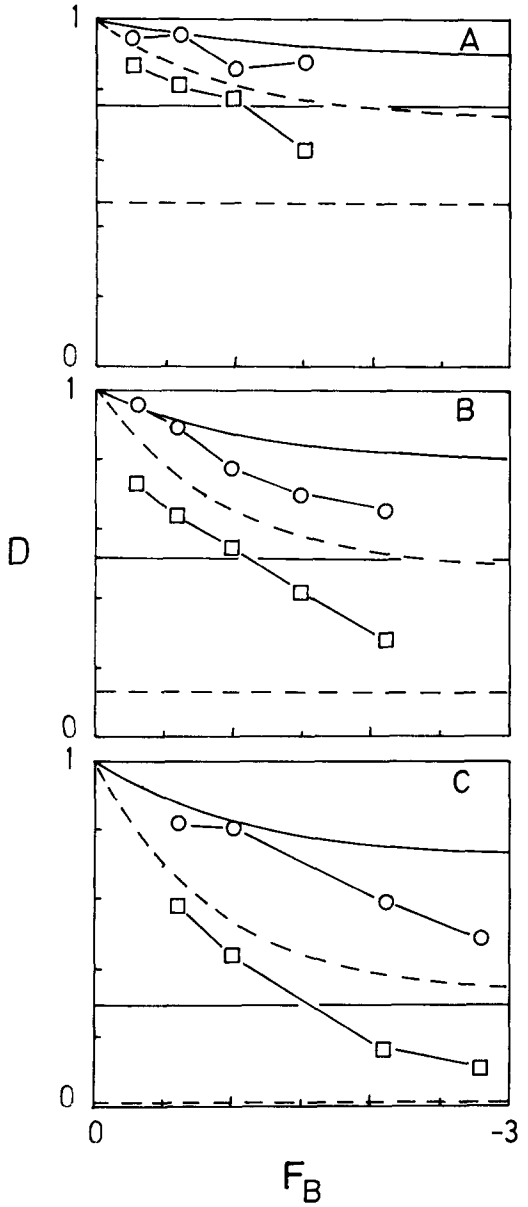

Fig. 3. Size-1 hexagons. Hexagon lateral diffusion disallowed. Relative diffusion coefficients, D_{nb} (○, and solid lines) and D_b (□, and dashed lines) as functions of F_B for $c = 0.5$. (A) $f_A = 0.207$. (B) $f_A = 0.400$. (C) $f_A = 0.558$. (i) Fast hexagon adsorption/desorption ($\tau_c \ll \tau_a$) uses the analytical expressions of Eqn. 3 (upper solid and dashed curves). (ii) $\tau_c \approx \tau_a$ (○,□). (iii) $\tau_c \gg \tau_a$ represented by a static hexagon distribution (lower solid and dashed horizontal lines).

$p \to 0$ with F_B not too weak, both diffusion coefficients will approach unity.

Figs. 5 and 6 are concerned with Size-2 hexagons. Fig. 5 is for non-binder concentration, $c = 0.5$, while Fig. 6 is for $c = 0.8$, and are the analogues of Figs. 1 and 2, respectively. A comparison of Fig. 5 with Fig. 1 (B, C and D) shows that D_{nb} displays, approximately, the same shape in corresponding cases, as functions of binding energy, F_B. D_b and f_A behave differently for Size-2 hexagons compared to Size-1 hexagons: f_A rises more rapidly with F_B for the larger hexagons, and D_b decreases more rapidly with F_B. The same behaviour can be seen in Fig. 6 (for $c = 0.8$) when it is compared to the results of Fig. 2 (B, C and D). These results suggest that, as functions of the binding energy, F_B, D_{nb} is much less dependent upon the size of adsorbed proteins bound to the interface than are D_b and F_A.

Fig. 7 shows the dependence of D_b and D_{nb} upon the average fraction of the surface covered by hexagons, f_A, for various values of F_B ranging from -0.1 to -2.8. It can be seen that Size-1 hexagons exhibit more scatter in the data than do Size-2 hexagons. This is to be expected and we shall discuss this in the next section. It might be noted that for both concentrations of binder, in the case of the larger hexagons, D_{nb} does not drop below 0.9 until f_A exceeds ~ 0.5 (Fig. 7B and D).

It is useful to show the dependence of D upon hexagon size, p and F_B, as a function of non-binder concentration, c. Figs. 8 and 9 show this for Size-0 ('hexagons' occupying only a single site ($n_H = 1$) on the lattice, so that this object is bound to only one binder or unbound) and for Size-2, respectively. Here, we chose $F_B = 1.5$ with $p = 0.1$ (Figs. 8 and 9A), and $F_b = -0.6$ with $p = 0.05$ (Fig. 9B), and plotted the results as a function of binder concentration, $1 - c$. Here we can clearly see the strong dependence of D_b upon the dynamics of the adsorption process. At binder concentration, $1 - c \approx 0.8$, for example, $f_A \approx 0.6$ in both cases shown in Fig. 9. D_b is reduced by a factor of 2 in

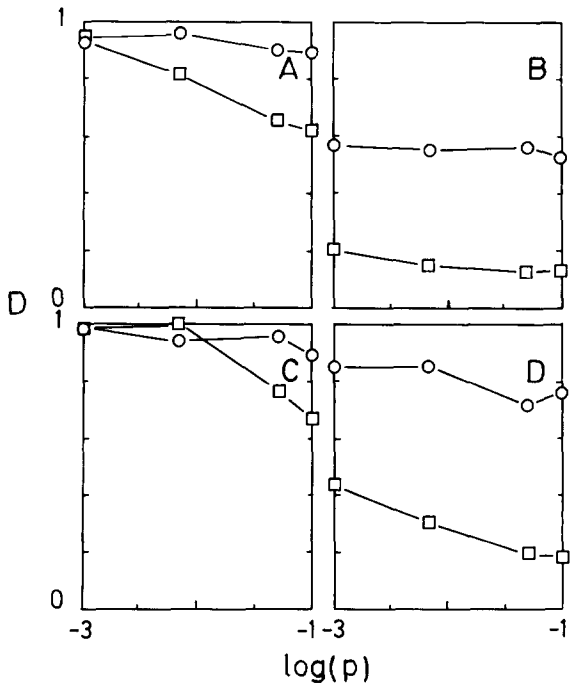

Fig. 4. Size-1 hexagons. Hexagon lateral diffusion disallowed. Relative diffusion coefficients, D_{nb} (○) and D_b (□), as functions of p, for various c and F_B. $c = 0.5$: (A) $F_B = -0.6$. (B) $F_B = -2.1$. $c = 0.8$: (C) $F_B = -0.6$. (D) $F_B = -2.1$.

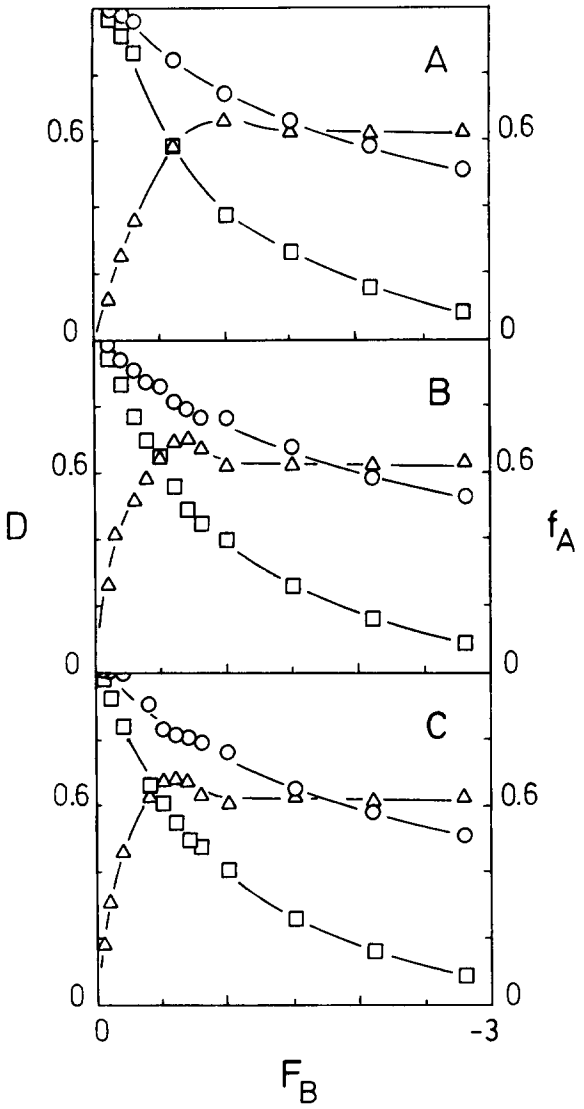

Fig. 5. Size-2 hexagons. Hexagon lateral diffusion disallowed. Relative diffusion coefficients, D_{nb} (○) and D_b (□), and f_A (△) as functions of F_B for $c = 0.5$. (A) $p = 0.007$. (B) $p = 0.05$. (C) $p = 0.1$.

the case in which the adsorbed configuration changes more slowly (Fig. 9A) than in the other case (Fig. 9B). The rate of change of the configuration of adsorbed hexagons will depend upon the probability of desorption, $\sim \exp(F_B)$, and that of adsorption, $\sim p(1 - f_A)$. The case of Fig. 9A will be more static than that of Fig. 9B and so D_b is lower in the former. D_{nb} must also be affected, but this is much less than a factor of 2, since non-binders can find their way in areas free of adsorbed hexagons or between bound binders under adsorbed hexagons. Fig. 8 illustrates the dependence of D upon size, and again shows that it is not only f_A which determines D, but also the rate at which configurations of adsorbed hexagons are changing. This point will be discussed in the next section.

Finally, we consider cases in which the adsorbed hexagons, together with the binders to which they are bound, can move laterally in the plane of the membrane. In this, we assume that the adsorbed hexagons diffuse at approximately the same rate as free binders or non-binders. If we first consider Size-1 hexagons, Fig. 10 (A and B) should be compared to Fig. 1 (B and D), while Fig. 10C should be compared to Fig. 2D. In the former cases the asymptotic value of f_A is higher by $\sim 10\%$ than in the latter case. This is probably due to the fact that we are allowing the bound hexagon configurations to anneal, so that hexagon-free areas are created onto which more hexagons can be bound. D_b is slightly higher in Fig. 10 (A and B) compared to Fig. 1 (B and D). The reason is that in this case there are many binders which are unbound. At low values of f_A many binders are free so that D_b is changed little even if the relatively small number of bound binders are allowed to move with the hexagons. At high values

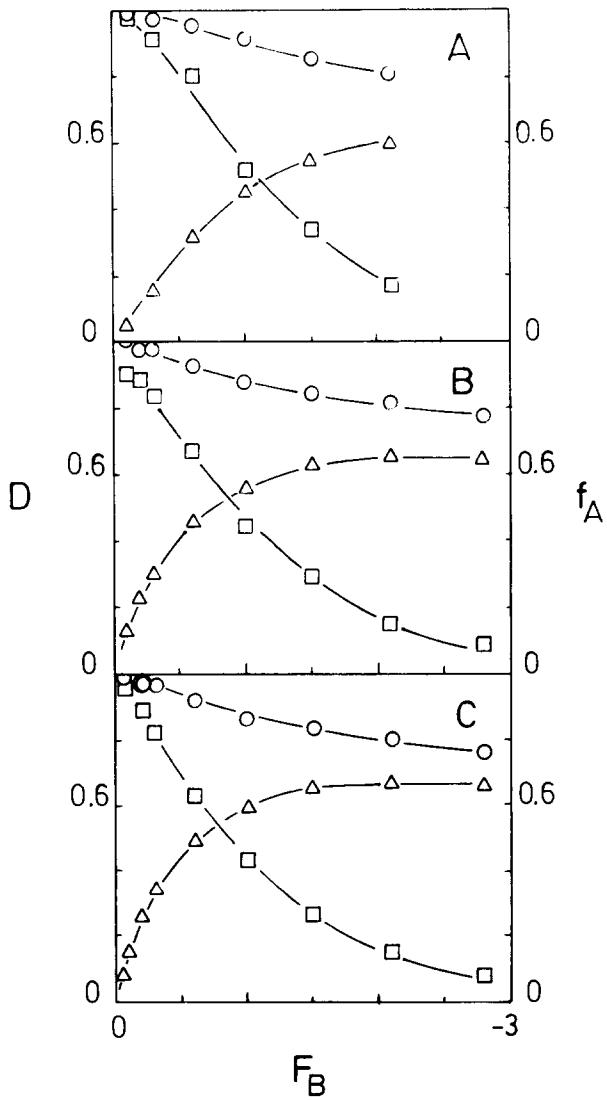

Fig. 6. Size-2 hexagons. Hexagon lateral diffusion disallowed. Relative diffusion coefficients, D_{nb} (○) and D_b (□), and f_A (△) as functions of F_B for $c = 0.8$. (A) $p = 0.007$. (B) $p = 0.05$. (C) $p = 0.1$.

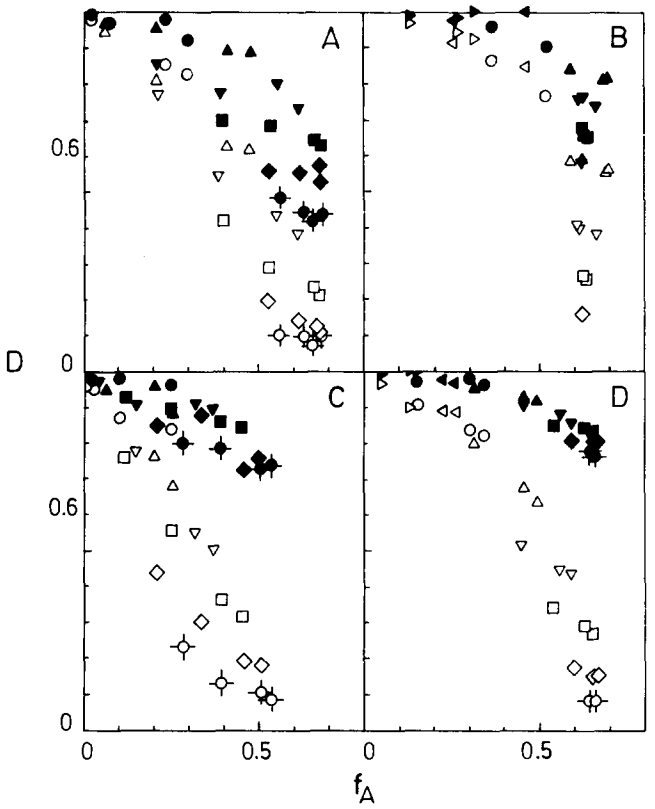

Fig. 7. D_{nb} (filled symbols) and D_b (unfilled symbols) as functions of f_A with hexagon lateral diffusion disallowed. (A) Size-1 with $c = 0.5$. (B) Size-2 with $c = 0.5$. (C) Size-1 with $c = 0.8$. (D) Size-2 with $c = 0.8$. F_B values are: -0.1 (▶,▷), -0.2 (◀,◁), -0.3 (●,○), -0.6 (▲,△), -1.0 (▼,▽), -1.5 (■,□) -2.1 (◆,◇) and -2.8 (●,○).

of f_A, the hexagons cannot move very much so that again D_b increases slightly. In the case of $c = 0.8$, however, there is a small number of binders, so that a relatively large fraction of them are bound except for very small values of f_A. Thus, if the hexagons can move, a larger change will be seen in D_b (Fig. 10C) when compared to the case in which they do not move (Fig. 2D). In all cases, D_{nb} increases slightly, as we would expect.

If we now consider Size-2 hexagons, Fig. 11 (A and B) should be compared to Fig. 6 (B and C). We chose $c = 0.8$ so that a large effect might be seen (above). For both cases we see essentially no change in f_A and D_{nb}, while D_b is ~ 50% higher in the case in which hexagons move.

Fig. 12 (A, B and C) should be compared to Fig. 7 (A, C and D). The first thing to notice is that the annealed system of moving hexagons can accommodate more hexagons than those with static distributions. This must be most noticeable when the hexagons are small, since the probability of creating free areas for hexagon adsorption is higher, the smaller the free area required. This is seen in comparing Fig. 12A and Fig. 7A. However, even if free areas are created by hexagon movement, f_A will not increase unless there are binders

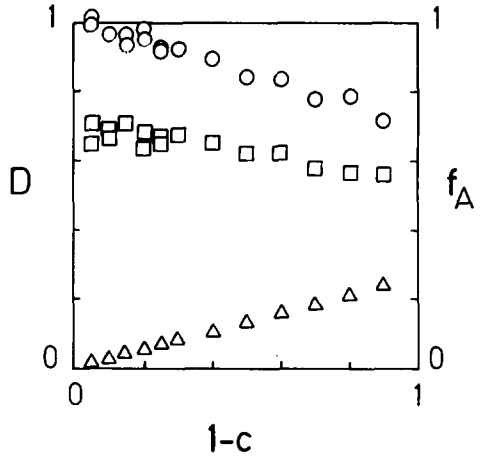

Fig. 8. Size-0 (single site) objects. Object lateral diffusion disallowed. Relative diffusion coefficients, D_{nb} (○) and D_b (□), and f_A (△) as functions of binder concentration, $1 - c$ for $F_B = -1.5$ and $p = 0.1$.

available to bind more hexagons. This effect is seen in Fig. 12B and Fig. 7C, where the binder concentration is $1 - c = 0.2$. No significant change is seen in D_{nb}, but D_b generally exhibits an increase in the case of hexagons which are allowed to move. This effect is most noticeable, as we would expect, for low binder concentration and smaller hexagons.

Our results suggest, therefore, that there will be a substantial advantage in measuring D_b instead of D_{nb}.

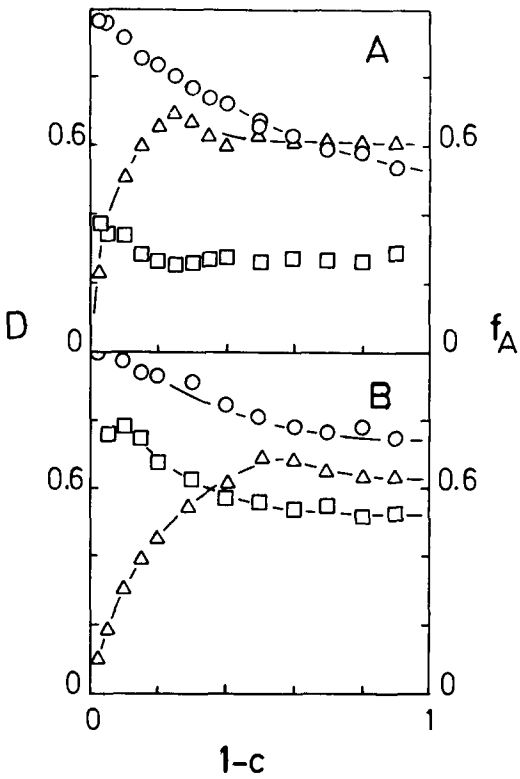

Fig. 9. Size-2 hexagons. Hexagon lateral diffusion disallowed. Relative diffusion coefficients, D_{nb} (○) and D_b (□), and f_A (△) as functions of binder concentration, $1 - c$. (A) $F_B = -1.5$, $p = 0.1$. (B) $F_B = -0.6$, $p = 0.05$.

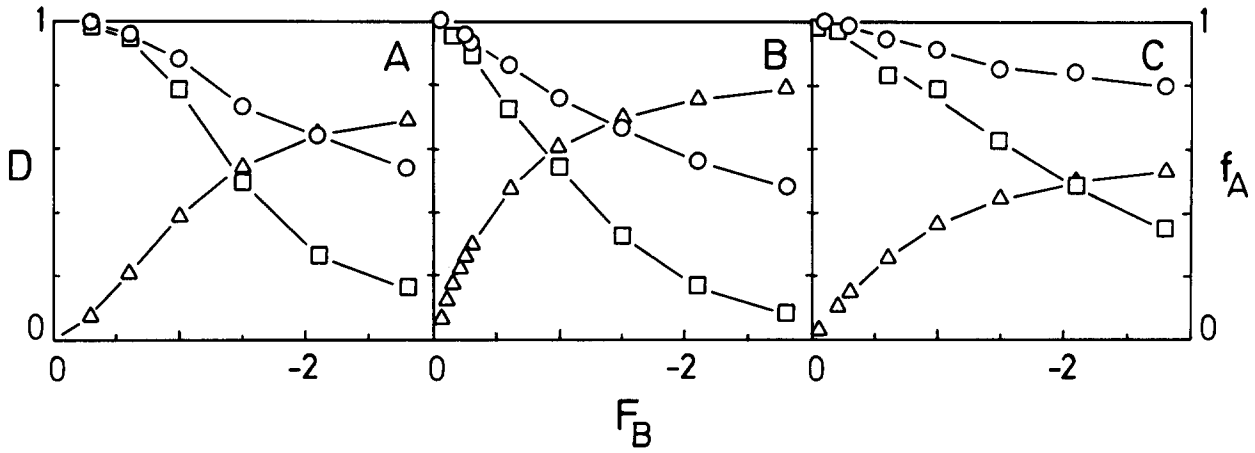

Fig. 10. Size-1 hexagons. Hexagon lateral diffusion permitted. Relative diffusion coefficients, D_{nb} (○) and D_b (□), and f_A (△) as functions of F_B. (A) $c = 0.5$, $p = 0.007$. (B) $c = 0.5$, $p = 0.1$. (C) $c = 0.8$, $p = 0.1$.

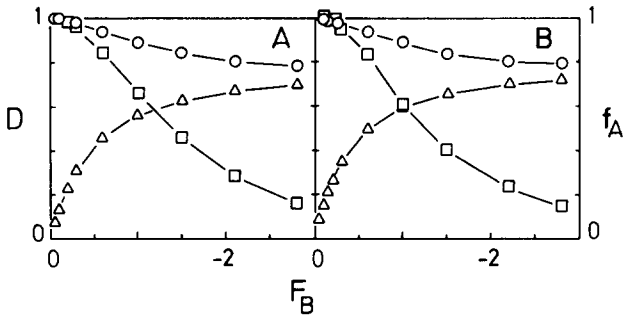

Fig. 11. Size-2 hexagons. Hexagon lateral diffusion permitted. Relative diffusion coefficients, D_{nb} (○) and D_b (□), and f_A (△) as functions of F_B for $c = 0.8$. (A) $p = 0.05$. (B) $p = 0.1$.

A measurement of both, however, should provide information on F_B as well as c, since the distribution of binders may not be symmetric with respect to both halves of the bilayer.

Conclusions

We have modelled the relative lateral diffusion of lipid molecules in a lipid bilayer or monolayer com-

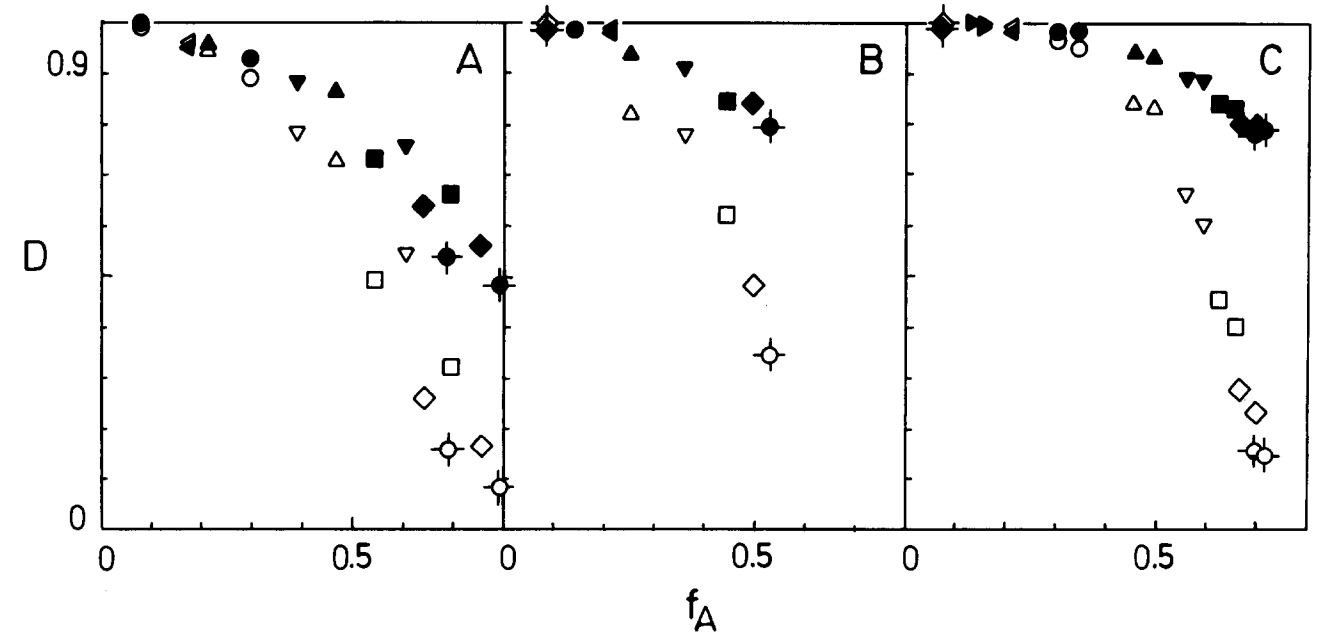

Fig. 12. D_{nb} (filled symbols) and D_b (unfilled symbols) as functions of f_A with hexagon lateral diffusion permitted. (A) Size-1 with $c = 0.5$. (B) Size-1 with $c = 0.8$. (C) Size-2 with $c = 0.8$. F_B values are -0.05 (♦,◇), -0.1 (▶,▷), -0.15 (◀,◁), -0.3 (●,○), -0.6 (▲,△), -1.0 (▼,▽), -1.5 (■,□), -2.1 (♦,◇), -2.2 (♦,◇) and -2.8 (●,○).

posed of two kinds of lipids, onto which macromolecules are adsorbing/desorbing. One type of lipid (binders) binds to the macromolecules, while the other type does not (non-binders). We have used a lattice model and have represented the 'footprint' of a macromolecule by a hexagon occupying n_H sites of the lattice. Each site of the lattice is considered to represent the cross-sectional area of a lipid molecule in a fluid phase with an area is ~ 0.6 nm^2. We have considered hexagons of two sizes: Size-1 for which $n_H = 7$ and Size-2 for which $n_H = 19$. These correspond to areas of $\sim 0.6\ n_H$ nm^2. We have also considered, only for comparison, Size-0 with $n_H = 1$. The model is characterized by three parameters: F_B, the free energy of binding between a hexagon and a binder; p, the probability that a hexagon centre will attempt to be adsorbed onto a randomly chosen site; and c, the concentration of non-binders.

We considered three time-scale regimes characterized by the times τ_a and τ_c, the times associated with lipid movement and protein adsorption or desorption: $\tau_c \ll \tau_a$, $\tau_c \approx \tau_a$ and $\tau_c \gg \tau_a$.

We carried out Monte Carlo computer simulations on a $(60)^2$ triangular lattice and obtained the dependence of the relative diffusion coefficient for binders and non-binders, D_b and D_{nb}, upon the parameters p and F_B for two concentrations, c. We calculated analytical expressions for D_b and D_{nb} for the case $\tau_c \ll \tau_a$.

We obtained the following results:

(i) For fixed p and c, the behaviour of D upon F_B can show a shoulder at small F_B if p is sufficiently small so that D remains near unity for a range of F_B. If p is sufficiently large, no shoulder appears but instead a steady decrease of D with increasing F_B is seen.

(ii) We have found, for the only case, $c = 0.5$, for which we performed the calculations, that, for a given F_B, the relative diffusion coefficients appear to satisfy the inequalities of Eqn. 10. The fastest diffusion appears to occur when the protein exchange on the membrane or monolayer surface is very rapid with $\tau_c \ll \tau_a$.

(iii) For given values of c and F_B, a study of D as a function of p shows that D_{nb} can remain very high (> 0.9), while D_b will, in general, quickly fall as p increases. We reiterate, therefore, that it is advisable to measure D_b in order to avoid the possibility that F_B is small so that $D_{nb} \approx 1$.

(iv) Lateral diffusion of adsorbed hexagons, whereby the hexagons and the binders to which they are bound diffuse as units, appears to have little effect upon D_{nb} compared to cases in which no lateral diffusion is permitted. This appears to be so even in the case of Size-1 hexagons. Such hexagon lateral diffusion has, however, a larger effect upon D_b. The magnitude of this effect can be seen, for example, for Size-2 hexagons when $c = 0.8$ and $f_A = 0.5$. In that case $D_b \approx 0.55$ if diffusion is disallowed while $D_b \approx 0.8$ if it is permitted. For Size-1 hexagons when $c = 0.5$ and $f_A = 0.5$, $D_b \approx 0.4$ (diffusion disallowed) and $D_b \approx 0.65$ (diffusion permitted). In general, bigger hexagons appear to give larger values of both D_b and D_{nb} than smaller hexagons, for a given value of f_A.

(v) Smaller hexagons appear to give rise to greater scatter of data points for both D_{nb} and D_b, for a given value of f_A, than do larger hexagons. The reason for this is, probably, that we can write D ($D = D_{nb}$ or D_b) as,

$$D \sim (A_0 - N_H A_H) D_{free} + N_H A_H D_{hex} + N_H A_H^{1/2} D_{hex\text{-}free}$$

$$\sim N_H [(A_1 - A_H) D_{free} + A_H D_{hex} + A_H^{1/2} D_{hex\text{-}free}] \qquad (11)$$

Here D_{free}, D_{hex} and $D_{hex\text{-}free}$ are the diffusion coefficients of lipids which are moving not under a hexagon, are moving under a hexagon, and are moving at the perimeter of a hexagon and sampling the free and the under-hexagon environments but in a random way. The first two quantities are weighted by the free area, $A_0 - N_H A_H$, and the area covered by hexagons, $N_H A_H$, where A_0 is the total area, A_H is the area per hexagon, $A_1 \equiv A_0/N_H$, and $N_H A_H / A_0 = f_A$. The third quantity must be weighted by the total perimeter length of the hexagons and this scales like $A_H^{1/2}$. It is the third term which can give rise to scatter in the values of D for fixed f_A because of the different paths that lipids diffusing in the neighbourhood of hexagon perimeters can take. As $A_H \to \infty$, however, the effect of the third term becomes irrelevant, so that scatter in plots such as that shown in Fig. 7 (A and C) vanishes. This can be seen in Fig. 7 (B and D).

Permitting the hexagons to diffuse laterally appears to reduce this scatter in data, as Fig. 12 shows.

In this paper we have studied the consequences of a very particular method of desorption. Each bound macromolecule-binder pair attempts to break, independently of what happens to other bound states on the same macromolecule. An alternative model could be to assume that desorption proceeds collectively, with all bound states becoming simultaneously unbound [32]. A comparison between the model presented here, an alternative model and other models is in progress.

Finally, we reiterate that, although some theoretical studies have been done on the effects of adsorbing macromolecules onto membranes, they have been concerned with calculating the concentration profiles of macromolecules on the membrane using diffusion equations and a knowledge of the diffusion coefficient [12,13]. The work presented here is, we believe, the first calculation of the relative diffusion coefficient itself.

Acknowledgements

It is a pleasure to thank Bonnie Quinn (T.P.I., St. Francis Xavier University) and K.S.S. Narayanan (Physics Department, Memorial University of Newfoundland) for their help and Thomas Bayerl (Dept. Physik, Technical University of Munich) for discussions. This work was supported in part by NSERC of Canada and St. Francis Xavier University.

References

1 Norde, W. (1986) Adv. Colloid Interface Sci. 25, 267–340.
2 Brash, J.L. and Horbett, T.A. (1987) Am. Chem. Soc. 343, 1–33.
3 Lee, S.H. and Ruckenstein, E. (1988) J. Colloid Interface Sci. 125, 365–379.
4 Meltzer, H. and Silberberg, A. (1988) J. Colloid Interface Sci. 126, 292–303.
5 Macritchie, F. (1989) Colloids Surf. 41, 23–34.
6 Lentz, B.R., Alford, D.R., Jones, M.E. and Dombrose, F. (1985) Biochemistry 24, 6997–7005.
7 Beschiaschvili, G. and Seelig, J. (1990) Biochemistry 29, 52–58.
8 Laroche, G., Dufourc, E.J., Pézolet, M. and Dufourc, J. (1990) Biochemistry 29, 6460–6465.
9 Tendian, S.W. and Lentz, B.R. (1990) Biochemistry 29, 6720–6729.
10 Egger, M., Heyn, C.P. and Gaub, H.E. (1990) Biophys. J. 57, 669–774.
11 Tilton, R.D., Gast, A.P. and Robertson, C.R. (1990) Biophys. J. 58, 1321–1326.
12 Elson, E.L. and Reidler, J.A. (1979) J. Supramol. Struct. 12, 481–489.
13 Koppel, D.E. (1981) J. Supramol. Struct. Cell Biochem. 17, 61–67.
14 Pink, D.A. (1985) Biochim. Biophys. Acta 818, 200–204.
15 Saxton, M.J. (1987) Biophys. J. 52, 989–997.
16 Scalettar, B.A., Abney, J.R. and Owicki, J.C. (1988) Proc. Natl. Acad. Sci. USA, 85, 6726–6730.
17 Minton, A.P. (1989) Biophys. J. 55, 805–808.
18 Abney, J.R., Scalettar, B.A. and Owicki, J.C. (1989) Biophys. J. 55, 817–833.
19 Abney, J.R., Scalettar, B.A. and Owicki, J.C. (1989) Biophys. J. 56, 315–326.
20 Pink, D.A. (1990) Computer Simulation of Biological Membranes, in Molecular Description of Biological Membranes by Computer Aided Conformational Analysis (Brasseur, R., ed.), Vol. 1, pp.151–170, CRC Press, Boca Raton.
21 Pink, D.A., Laidlaw, D.J. and Chisholm, D.M. (1986) Biochim. Biophys. Acta 863, 9–17.
22 Saxton, M.J. (1989) Biophys. J. 55, 21–28.
23 Saxton, M.J. (1990) Biophys. J. 58, 1303–1306.
24 Eggl, P., Pink, D., Quinn, B., Ringsdorf, H. and Sackmann, E. (1990) Macromolecules 23, 3472–3480.
25 Shirahama, H., Lyklema, J. and Norde, W. (1990) J. Colloid Interface Sci. 139, 177–187.
26 Raudino, A., Castelli, F. and Gurrieri, S. (1990) J. Phys. Chem. 94, 1526–1535.
27 Saffman, P.G. and Delbrück, M. (1975) Proc. Natl. Acad. Sci. USA, 72, 3111–3113.
28 Marçelja, S. (1974) Biochim. Biophys. Acta 367, 165–176.
29 Pink, D.A., Green, T.J. and Chapman, D. (1980) Biochemistry 19, 349–356.
30 Vaz, W.L.C., Goodsaid-Zalduondo, F. and Jacobson, K. (1984) FEBS Lett. 174, 199–207.
31 Páli, T. and Horváth, L.I. (1989) Biochim. Biophys. Acta 984, 128–134.
32 MacNeil, M.G. (1991) Models of Two-Dimensional Tracer and Binder Lateral Diffusion through a Background of Adsorbing and Desorbing Particles. Thesis. St. Francis Xavier University.